Available online at www.sciencedirect.com

ScienceDirect

Procedia Materials Science 3 (2014) 1453 – 1458

Procedia Materials Science

www.elsevier.com/locate/procedia

20th European Conference on Fracture (ECF20)

On fatigue behavior of two spring steels. Part I: Wöhler curves and fractured surfaces

Donka Angelova, Rozina Yordanova, Tsvetelina Lazarova, Svetla Yankova *

University of Chemical Technology and Metallurgy, St. Kliment Ohridski 8, Sofia 1756, Bulgaria

Abstract

Symmetric fatigue in two spring steels is investigated in three groups of specimens. One of the groups (Steel EN10270-1SH/ DIN 17223C – C 0.82%, Mn 0.76%, Si 0.26%) has experienced rotating-bending fatigue in air, and the other two groups (Steel BS250A53/ DIN 55Si7 – C 0.56%, Mn 0.81%, Si 1.85%), torsion fatigue in-air and corrosion environment. Fatigue life-time data are obtained for both spring steels, and their corresponding Wöhler curves plotted and mathematically described. Surface short fatigue cracks are observed from origin to fracture by using acetate-foil replication technique, and their length, *a,* measured at the corresponding number of fatigue cycles, *N.* Those data are presented in plots "Crack lengths, *a* – Cycles, *N*" and a comparison made between both the steels. The fractured surfaces of all specimens have been studied and analyzed by the scanning-electron microscopy methods.

Selection and peer-review under responsibility of the Norwegian University of Science and Technology (NTNU), Department of Structural Engineering

Keywords: rotating-bending fatigue; torsion fatigue; Wöhler curve; short-fatigue-crack growth; fatigue-crack path

1. Introduction

Spring steel is a low-alloy, medium-carbon steel or high-carbon steel with a very high yield strength, allowing objects made of spring steel to return to their original shape despite significant bending or twisting. Required properties of such a steel vary accordingly. However, whatever its application can be, it is certain that a high stress during cyclic loading and prolonged reliability should be required. The fatigue strength of a spring steel is affected by many factors, such as material, shape, loading, environment. Generally fatigue failure occurs by propagation of

* Corresponding author. Tel.: +359 879 601 737.
E-mail address: donkaangelova@abv.bg

Selection and peer-review under responsibility of the Norwegian University of Science and Technology (NTNU), Department of Structural Engineering
doi:10.1016/j.mspro.2014.06.235

subcritical cracks ranged from several microns to a few hundred microns, Suresh (1998). Fatigue crack growth characteristics are normally expressed by the relation between stress intensity factor range and crack growth rate. It is generally recognized that the linear fracture mechanics allows to be defined the threshold condition under which a fatigue crack can propagate as a large crack. In high strength materials as spring steels some physically small cracks can lead to fatigue fracture. But in all cases fatigue failure begins from much smaller cracks known as short cracks originating in one grain or at flows, i.e. as nonmetallic inclusions; these cracks can be surface cracks or below-surface ones and there exist different mathematical models (from linear fracture mechanics ones) of their behavior, Miller (1991), Suresh (1998).

2. Experimental work

2.1. Material and specimens

For this study two spring steels were used: Steel EN10270-1SH/ DIN 17223C (Steel A) for conducting own fatigue experiments, Nikolova et al. (2014); and BS250A53/DIN 55Si7 (Steel B), for using some already published results, Murtaza (1992), Yordanova (2003), and making comparative analysis with Steel A. Both, their microstructure and chemical compositions, are shown in Fig. 1 and Table 1.

EN 10270-1 SH (DIN 17223C) is high strength eutectoid spring steel, with a microstructure showing alternating ferrite and cementite lamellas. This steel is mainly used for manufacturing springs and other elastic elements. The biggest Bulgarian spring producer is the Company Feder Universal & Co Ltd Bulgaria (http://www.feder-u.com/) using imported spring steels with main supplier TREFILAC, France.

Steel BS 250A53 (DIN 55Si7) is silico-manganese spring steel.This is a high carbon low alloy steel in the quenched and tempered condition used for the manufacture of railway track clip fastenings. Steel B experienced specific treatment, described by Murtaza (1992) as follows. The hardening was conducted by heating the material to an austenitising temperature of 950^{o}C for 15 minutes followed by quenching in oil. Tempering was then carried out at a temperature of 450^{o}C for 30 minutes. The microstructures obtained after the given heat-treatments were analyzed by an image analysis system. A large number of non-metallic inclusions were seen. The average prior austenite grain sizes were found to be around 30.10^{-6} m and 60.10^{-6} m for standard and large grain size, respectively.

Specimens of Steel A and Steel B are machined in hour-glass shape, and shown in Fig. 2.

2.2. Equipment and testing

Steel A. Twelve hourglass-shaped specimens were subjected to symmetric cyclic rotating-bending fatigue (RBF) to fracture at different stress ranges ($\Delta\sigma$ = 800, 1000, 1200, 1400 and 1500 MPa) and at the following testing conditions: R=-1, f=11 Hz, air environment and room temperature. Tests were performed on a table model Fatigue Rotating Bending Machine, FATROBEM-2004, designed and assembled in “Fracture and Fatigue” Laboratory in the University of Chemical Technology and Metallurgy–Sofia, UCTM, Fig. 2. A Scanning electron microscope (SEM) was used for having studied both, microstructure and fatigue-fractured surfaces, in the Laboratory LETAM (Laboratory of Study of Textures and Application to Materials), Paul Verlaine University–Metz, France.

Steel B. Fourteen hourglass-shaped specimens were used in fatigue tests conducted by Murtaza in the Fracture and Fatigue Laboratory of the Institute SIRIUS, The University of Sheffield. The tests were carried out under fully reversed torsion loading conditions (TF) and frequency f=5 Hz for two sets of stress ranges applied in two different environments: in-air fatigue tests at $\Delta\tau$ = 915, 1080, 1106 MPa (respectively $\Delta\gamma$ = 1.24, 1.57, 2.22%); and corrosion fatigue tests in 0.6M NaCl at $\Delta\tau$ = 404, 601, 815, 900 MPa (respectively $\Delta\gamma$ = 0.49, 0.73, 1.03, 1.2 %).

2.3. Crack Growth Monitoring Method

A replication technique was used for short fatigue-crack growth monitoring according to technical standards, Dowling (2006). This method consists of making a replica (stamp) of specimen’s surface and subsequent monitoring of crack length and its propagation. Replicas are taken onto two mutually opposite specimen surfaces, which ensures full coverage of its hourglass working area.

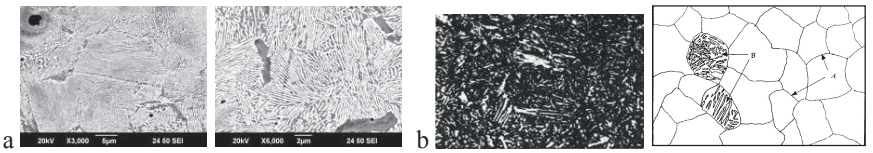

Fig. 1. Microstructures of: (a) Steel A; (b) Steel B with schematic presentation (.A-Prior austenite grain boundaries, B-Martensite laths).

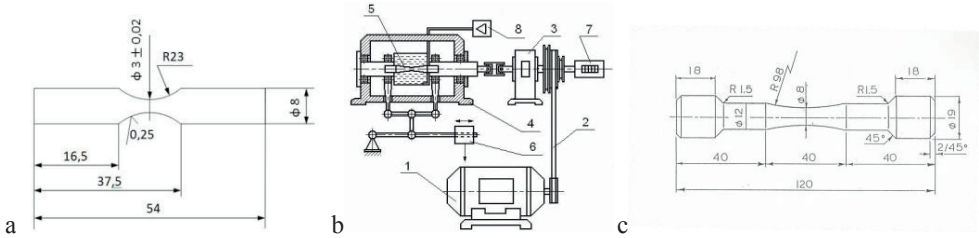

Fig. 2. Specimen geometry and fatigue equipment: (a) steel A specimen; (b) fatigue machine FATROBEM 2004; (c) Steel B specimen; FATROBEM 2004 - electric engine 1, driving belt 2, ball-bearing unit 3, testing box 4, specimen 5, device for loading 6, counter 7, device for circulation and aeration of corrosion agent 8.

Table 1. Chemical composition and mechanical properties of examined steels.

Chemical composition. wt %											
	C	Mn	P	S	Si	Al	Cr	Ni	Cu	Mo	N_2
EN 10270-1 SH (DIN 17223C)	0.819	0.760	0.010	0.001	0.257	0.034	0.251	0.016	0.011	0.003	0.005
BS 250A53 (DIN 55Si7)	0.52-0.57	0.8-1.0	≤0.05	≤0.05	1.8-2.1	-	0.2-0.3	≤0.3	-	0.01-0.06	-
Mechanical properties											
	Ultimate tensile strength, MPa				Yield stress, MPa				Elongation, %		
EN 10270-1 SH (DIN 17223C)	1522				1217						
BS 250A53 (DIN 55Si7)	1610				1440				9.3		

Replication material used is synthetic acetate film type "Agar scientific". After each experiment all replicas with cracks are subjected to closer monitoring and then the crack lengths are measured at the corresponding number of cycles at their taking. Measurement of cracks is done by using an optical microscope.

3. Results and discussion

All specimens of Steels A (BRF) and B (TF) were tested to fracture. The corresponding Wöhler curves were obtained by applying the well-known standard procedure and data recording; the curves are plotted and presented with their analytical models in Fig. 3 (for Steel A) and in Fig. 4a (for Steel B) and together for comparison - in Fig. 4b.

In Fig. 3 are also shown fractographic images of the fractured surfaces of some tested specimens; the chosen specific areas of the fractured surfaces are: crack initiation zone, crack propagation zone and zone of final fracture. The specimens tested at stress range $\Delta\sigma$ = 1500 MPa (Specimens 10 and 12) show several crack initiation zones which correspond to the shorter lifetimes of these specimens in comparison with the rest from the same group A, Nikolova et al. (2013). Marked numbers of specimens and the corresponding explanations of the fractografic images of their fractured surfaces shown in Fig. 3 are presented in Table 2 in terms of providing a better understanding of the whole picture.

By analogy the corresponding Wöhler curves for Steel B in air and aggressive environment are shown in Fig.4a together with characteristic areas with surface short cracks; these cracks are observed on the hourglass specimen surfaces, corresponding to given numbers of cycles from cracks originating through their propagation to the final stage of near-failure moments before complete specimen fracture. A comparison between fatigue behaviour of

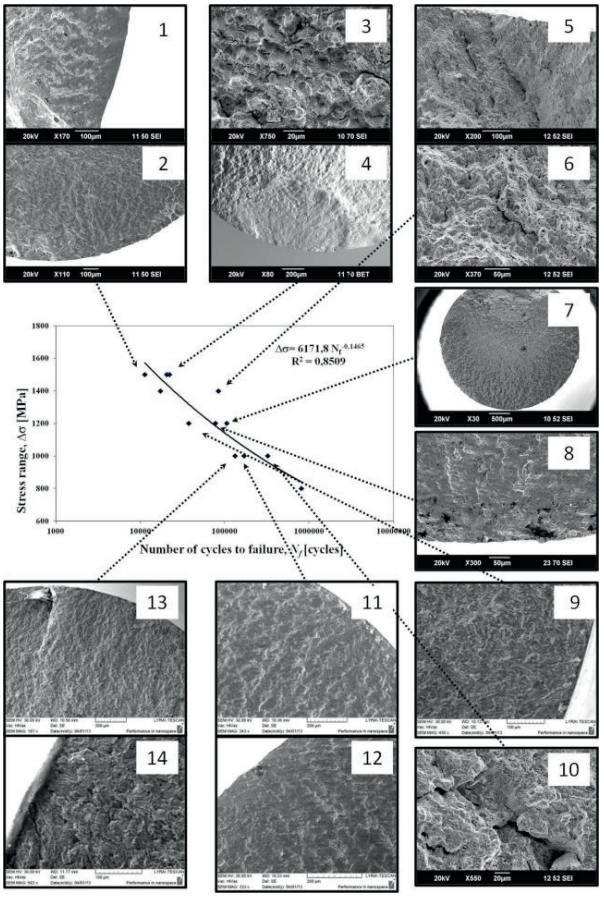

Fig. 3. Wöhler curve of Steel A and characteristic areas of the fractured specimen surfaces corresponding to some stress ranges.

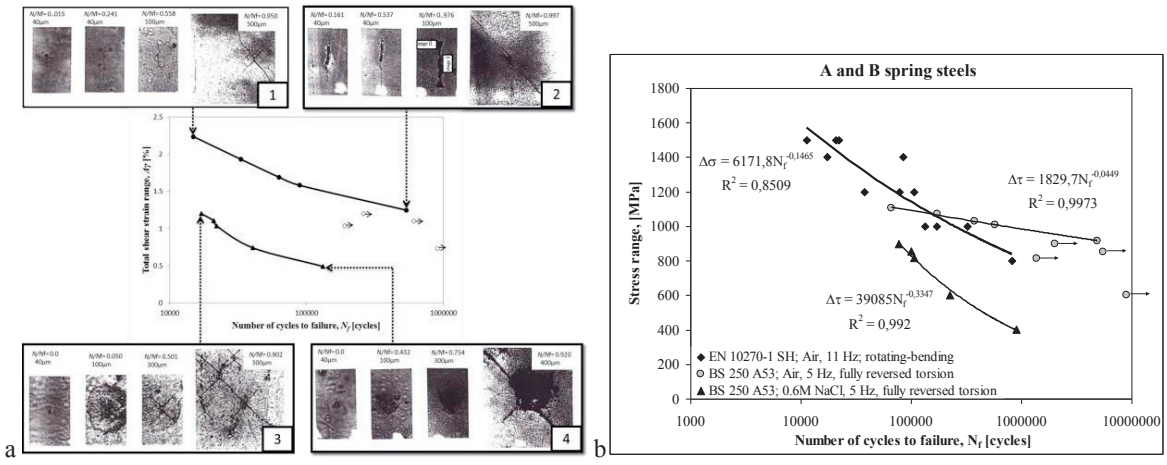

Fig. 4 Wöhler curves: (a) Steel A and characteristic areas with short cracks on the hourglass specimen surfaces, corresponding to given number of cycles. The higher curve shows in-air fatigue, $\Delta\gamma = 9.86N_f^{-0.136}$, and the lower curve - corrosion fatigue, $\Delta\gamma = 73.31N_f^{-0.368}$; (b) comparison between Wöhler curves of both steels.

Table 2. Stress-Cycles-Fractographic characteristics connected with the Wöhler curve of Steel A.

Image	Marked number of specimens	Δσ, MPa	Fractographic characterization	Image	Marked number of specimens	Δσ, MPa	Fractographic characterization
1	12	1500	Crack initiation zone	8	6	1200	MnS inclusion at crack initiation zone
2	12	1500	Crack initiation zone/Crack propagation zone	9	7	1200	Crack initiation zone
3	10	1500	Zone of final failure	10	2	1000	Microcracks – zone of final failure
4	10	1500	Crack initiation / propagation zone	11	3	1000	Crack initiation zone
5	8	1400	Zone of final failure	12	3	1000	Crack initiation zone
6	8	1400	Microcracks – zone of final failure	13	4	1000	Crack propagation zone/Zone of final failure
7	5	1200	Fracture surface	14	4	1000	Crack initiation zone

Steels A and B in stress terms (although presented in $\Delta\sigma$ and in $\Delta\tau$) Fig. 4b, shows a pronounced influence of material nature and of different kind of fatigue condition - RBF and TF. At the same time the strongest factor is obviously the surrounding environment, which is clearly focused on the corresponding Wöhler curve - the lowest one in Fig. 4b.

Cracks development and paths can be observed in Fig. 5. Fractured surfaces of Specimen 7 are presented in Fig. 5a. By performing closer observation and analysis of the shown fractured surface a few crack initiation zones are found and three of them are chosen and indicated by black dashed-line ovals. The magnified images of these zones are shown separately in the black boxes in the same figure. It has been found that in the early stages of fatigue process the three cracks (originated from different spots) propagated independently from each other. However, in the further stages of fatigue development an interaction of the three cracks is observed, causing exhaustion of local plasticity and crack-merging process. The merging process gradually involves other cracks and finally a main crack is formed leading to the complete fracture of Specimen 7. The observed cracks interaction on the fractured surface of Specimen 7 also can be indirectly confirmed by replica monitoring of surface propagation of short fatigue cracks, Fig. 6a. Figures 4a, 5b, 6b show fatigue cracks growth in the specimens of Steel B, tested under different stress ranges. The major crack propagation at $\Delta\tau$ = 915 MPa and in-air environment can be microstructully seen in Fig. 5b; in comparison to it the observed corrosion fatigue in the specimen under the highest stress range of $\Delta\tau$=900 MPa (Steel B), Fig. 4a, shows intense interaction between all the surface short cracks.

Data from replica monitoring of surface short cracks propagation (in Specimens 7 ($\Delta\sigma$ = 1200 MPa) and 9 ($\Delta\sigma$ = 1400 MPa) obtained by use of metallographic microscopy) are plotted as "Crack length, *a* -Numbers of cycles, *N*" and shown in Fig. 6a. In both cases the major cracks from the families "Major crack - Secondary cracks" have originated first. It can be seen that the major crack of Specimen 9 (tested at higher stress range) has initiated in an earlier stage in comparison to the initiation stages of all the secondary cracks. At the same time the major crack and all the secondary cracks in Specimen 7 show small difference at the number of cycles to initiation, almost parallel propagation and a kind of competition between the secondary cracks for merging their propagation paths with that of the major crack; also the major crack length is smaller than that of Specimen 9 which is tested at higher stress range. The surface of Specimen 7 whole-working area shows (by observation after specimen's fracture) unusual roughness, probably due to the polishing of the specimen; it confirms the especially strong influence of the surface-condition factor on fatigue behaviour.

The curves "Crack length – N umbers of cycles" for B steel are plotted in Fig. 6b. They show a major crack and only a few secondary cracks in each family "Major crack - Secondary cracks" corresponding to a given stress range. An exception is the family "Major crack – Secondary cracks" at $\Delta\tau$ =900 MPa in corrosion environment with several secondary cracks; this can be seen clearly in Fig. 4a on the corresponding microstructure that is result of application of $\Delta\gamma$ =1.2% ($\Delta\tau$ =900 MPa) at N/N_f =0.902. The family "Major crack–Secondary cracks" at $\Delta\tau$ =817 MPa in corrosion environment has more secondary cracks than those at $\Delta\tau$ =404 MPa and $\Delta\tau$=601 MPa, Fig. 6b. At the same time the two families "Major crack – Secondary cracks" at $\Delta\tau$ =817 MPa and 900 MPa having more secondary cracks are located very closely, which shows than above $\Delta\tau$ =817 MPa surface short cracks propagation and paths, Fig. 6b, look like those of the family "Major crack – Secondary cracks" of Specimen 7 ($\Delta\sigma$=1200 MPa), Steel A, Fig. 6a. This means that nature of material is of great importance, but varying with fatigue loading and kind of scheme, as well as with environment and surface condition, it is possible to observe (it can lead to) a similar short fatigue crack behaviour.

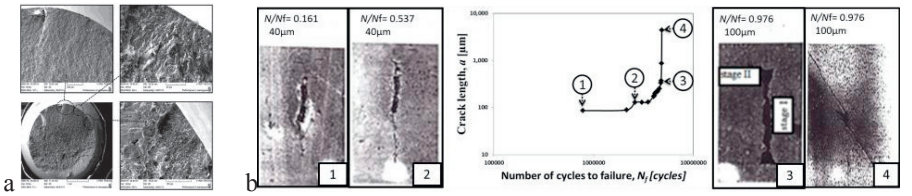

Fig. 5. Images of failure development and fractured surfaces: (a) fractographic observations of the fractured surfaces of Specimen 7 ($\Delta\sigma$=1200 MPa) from Steel A specimens; (b) crack development at $\Delta\tau$ = 915 MPa, Steel B, Air.

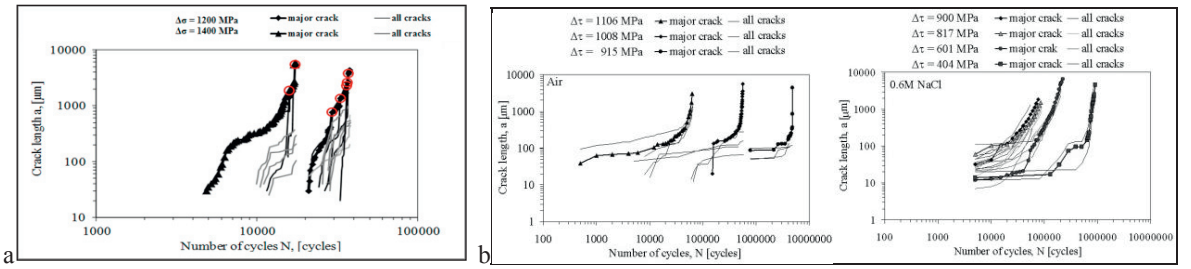

Fig. 6. Presentation "Crack length, *a* - Numbers of cycles, *N*": (a) Streel A, Specimen 7 ($\Delta\sigma$ =1200 MPa) and Specimen 9 ($\Delta\sigma$ =1400 MPa); (b) Steel B, Specimen sets tested in-air and corrosion environment.

4. Conclusions

Fatigue behavior of two different spring steels was investigated: Steel EN10270-1SH/ DIN 17223C (Steel A) for own fatigue experiment; and BS250A53/DIN 55Si7 (Steel B) with already published fatigue data and for comparison with Steel A. Steel A is subjected to symmetric rotating bending fatigue in air, and Steel B - to fully reversed torsion fatigue in-air and corrosion environment.

The presentation of the plotted Wöhler curves of both steels show that loading, surface condition and environmental factors are ones of the most influential factors. In Steel A for one of the highest stress range ($\Delta\sigma$ = 1200 MPa) and at rough specimen surface, the surface short-fatigue-cracks development and observed mictrostructures show initiating, propagating and interaction between major and many secondary cracks in its vicinity, leading to exhaustion of local plasticity, crack merging and complete failure. In Steel B a similar situation can be observed only in corrosion environment and above certain high stress range ($\Delta\tau$ = 817 MPa). All this should be taken into consideration at choosing steels for different applications under fatigue conditions.

Acknowledgements

This study was supported by the Scientific Research Center at UCTM – Sofia, Bulgaria.

References

Dowling N., 2006. *Mechanical Behaviour of Materials*, Prentice-Hall, New Jersey, USA.
Miller K. J., 1991. Metal Fatigue – Past, Current and Future. Proc. Inst. Mech. Engrs, London.
Murtaza G., 1992. Corrosion Fatigue Short Crack Growth Behaviour in a High Strength Steel. PhD thesis-University of Sheffield.
Nikolova L., Yordanova R., Yankova Sv., 2013. Wöhler curve and fatigue characteristics of spring steel. Engineering Sciences 2, 39-47.
Nikolova L., Yordanova R., Angelova D., 2014. Investigation on Fatigue Behavior and Fatigue Crack Growth of Spring Steel. Part I. Wöhler Curve and Fracture Surfaces. Journal of Chemical Technology and Metallurgy, 49, 1, 23-28.
Suresh S., 1998. Fatigue of Materials. Cambridge Univ. Press, Cambridge, UK.
Yordanova R., 2003. Modeling of fracture process in low-carbon 09Mn2 steel on the bases of short fatigue crack growth experiments. Comparative analyses on the fatigue behavior of other steels, PhD Thesis, University of Chemical Technology and Metallurgy, Bulgaria.